Deconvolution of lifetime broadening at rare-earth L_{III} edges compared to resonant inelastic x-ray scattering measurements

P. W. Loeffen
European Synchrotron Radiation Facility, Boîte Postale 220, F-38043 Grenoble Cédex, France

R. F. Pettifer
Department of Physics, University of Warwick, Coventry CV4 7AL, United Kingdom

S. Müllender and M.A. van Veenendaal
European Synchrotron Radiation Facility, Boîte Postale 220, F-38043 Gremble, Cédex, France

J. Röhler
Universität zu Köln, Physikalisches Institut, Zülpicher Strasse 77, D-50937 Köln, Germany

D. S. Sivia
Rutherford Appleton Laboratory, Chilton, Didcot, Oxford OX11 0QX, United Kingdom
(Received 17 July 1996)

The lifetime broadening of some rare-earth L_{III}-edge x-ray absorption spectra (XAS) is partially removed by deconvolving high quality data. The ligand field splitting of dipolar resonances is clearly resolved. Exposed pre-edge structure is compared to atomic multiplet calculations of the $2p \rightarrow 4f$ quadrupolar excitations. Ratios are thereby determined for the quadrupolar/dipolar oscillator strengths. Deconvolved XAS data of $Ho(NO_3)_3$ are compared to inelastic x-ray scattering measurements showing experimentally that the latter cannot reproduce a narrowed XAS. [S0163-1829(96)05546-4]

An inherent limitation of x-ray absorption spectroscopy (XAS) of deep core holes has remained the lifetime broadening. This is of significance to a wide scientific community that exploits XAS. For the $2p$ core holes of rare earths (RE's) this broadening is $3.5 \rightarrow 4.5$ eV.[1] The existence of pre-edge features at the $L_{II,III}$ edges was therefore first demonstrated via magnetic x-ray scattering[2,3] and x-ray dichroism.[4–7] They were attributed to electric quadrupolar excitations into $4f$ states that, although being weak and therefore undetectable in XAS, can be observed due to their strong dichroism.[6,7] Other techniques have also been explored in order to demonstrate their presence in a more direct way. Hämäläinen *et al.*[8] measured the inelastic x-ray scattering (IXS) of $Dy(NO_3)_3$ by measuring a narrow component of the $3d \rightarrow 2p$ emission spectrum at fixed energy. In a more recent IXS study of Gd garnet, Krisch *et al.*[9] distinguished individual resonances at the L_{III} threshold by measuring components of the emission spectrum at fixed energy transfer. Although these techniques show well-separated pre-edge structure, none of them removes the core hole lifetime broadening. In the former IXS technique, narrow features are observed but these are an arbitrary combination of intermediate and final state structures[10,11] where the final state contains a hole in a shallower core level. Therefore such IXS spectra cannot be viewed as the XAS spectrum with a reduced lifetime broadening as was first claimed.[8,12] Furthermore, besides their complex interpretation, these spectra are difficult to obtain. Here we show that XAS spectra with an effective reduced lifetime broadening can be obtained by a deconvolution procedure using high quality XAS data that exploit the stability of the new generation of x-ray sources and monochromators. We justify this procedure with an error estimation from information theory and by a comparison of the deconvolved L_{III}-edge spectra from five RE compounds, $Gd_3Ga_5O_{12}$, $Dy(NO_3)_3$, $Ho(NO_3)_3$, $Er_3Ga_5O_{12}$, and Er_2O_3, with numerical simulations of the electric quadrupole XAS spectra. Using this method, we are able to show experimentally with data obtained for $Ho(NO_3)_3$ that IXS does not measure a *narrowed* XAS spectrum. This paper shows that much more detailed information can be extracted from high quality XAS spectra than was generally considered possible.

All measurements were performed on the bending magnet beam line BM29 at the ESRF. The x rays were monochromatized using flat Si[220] crystals which gave a measured resolution at full width at half maximum (FWHM) of $\Delta E/E = 6 \times 10^{-5}$ (0.5 eV at the Ho L_{III} edge). The beam was unfocused and the spot size was defined by slits to be ~ 1 mm vertical by 10 mm horizontal at the sample producing an incident flux of 10^{10} photons/sec (for 100 mA electron beam current).

The IXS measurements of powder $Ho(NO_3)_3$ used a spherically bent Si[444] analyzer in near back reflection ($\theta_B = 88.5°$) Rowland's geometry to image the Ho $L\beta_2$ emission spectrum at ~ 7911 eV. The sample was an undiluted pellet and was oriented at 60° to the incoming beam to create a 20 mm extended source in the horizontal. The radiation scattered at 90° in the horizontal plane was energy dispersed by the analyzer and several eV were thereby imaged onto a position sensitive detector (PSD). The energy resolution of the image was dominated by the spatial resolution of the PSD to be ~ 0.25 eV.

XAS spectra were recorded in transmission over 400 eV centered on the L_{III} edges with a sampling interval of 0.1 eV (typically 3 h total measurement time). The XAS spectra were deconvolved with a Lorentzian response function by applying Stoke's theorem. Fast Fourier transforms (FT's) of the spectra were optimally filtered using the Wiener method and divided by the analytical form of the Lorentzian FT, $F(x)=\exp(-\frac{1}{2}\Gamma|x|)$, where Γ is the FWHM of the Lorentzian. Each deconvolution was performed on a minimum of four experimental spectra to check for consistency. The deconvolution was also performed using the maximum entropy method but no significant differences were observed with either data sets or deconvolution methods.

The XAS spectra presented in this paper were partially deconvolved by Lorentzians with widths not more than $\Gamma=3$ eV. This value of Γ is considerably less than the anticipated L_{III} natural lifetime widths of the RE compounds considered [ranging from 4.01 eV for Gd to 4.35 eV for Er (Ref. 1)] but a much larger value was unjustified by the analysis below. Practical limits on deconvolution can be set from information theory, and in particular the Shannon-Hartley theorem.[13] The latter theorem yields $I_{\max}=B\ln(1+S/N)$, with $I_{\max}$ the maximum information rate through a continuous channel disturbed by white Gaussian additive noise, B the bandwidth of the channel, and S/N the signal-to-noise power ratio. While this theorem is proved for a restrictive set of circumstances, it is known that real nonoptimally coded signals (such as a spectrum) also transport information with the same form of S/N and bandwidth dependency. Deconvolution is a mathematical operation which under optimal conditions conserves information. Equating the information rate before and after deconvolution dictates that we pay for an increase in bandwidth via a reduction in the S/N power ratio. The power spectra of the data exhibit an exponential decay characterized by Γ_1 which is inversely proportional to the bandwidth. Deconvolution of a Lorentzian broadening, Γ, multiplies B by $\Gamma_1/(\Gamma_1-\Gamma)$ with a decrease in S/N such that

$$\left[\frac{S}{N}\right]_2=\left[\frac{S}{N}\right]_1^{(\Gamma_1-\Gamma)/\Gamma_1}, \tag{1}$$

where the subscripts 1 and 2 refer to the measured and deconvolved spectra, respectively. In the case of $Ho(NO_3)_3$ the power spectrum of the data is characterized by $\Gamma_1=6.2$ eV and power $S/N=10^8$. A deconvolution of $\Gamma=3$ eV yields a final standard error of the data of $\sim$1%. It is thus only possible to successfully perform this deconvolution exercise with high quality experimental data.

Figure 1 shows the measured L_{III} XAS data of five RE materials and the same spectra after partial deconvolution by a Lorentzian of width $\Gamma=3$ eV. The deconvolution reveals striking new structure in the spectra that was formerly concealed by the $2p$ lifetime broadening. In particular, the splitting of the dipolar $|2p^6 5d^0\rangle\rightarrow|2p^5 5d^1\rangle$ resonance in Er_2O_3 is clearly resolved to be 3.4 eV. The splitting arises because the Er_2O_3 crystal environment[14] exerts a field of cubic symmetry on the Er atoms which projects the $5d$ orbitals into two distinct representations of t_{2g} and e_g symmetry. The measured peak separation can be used to find the cubic ligand field splitting (denoted as $10Dq$).[15]

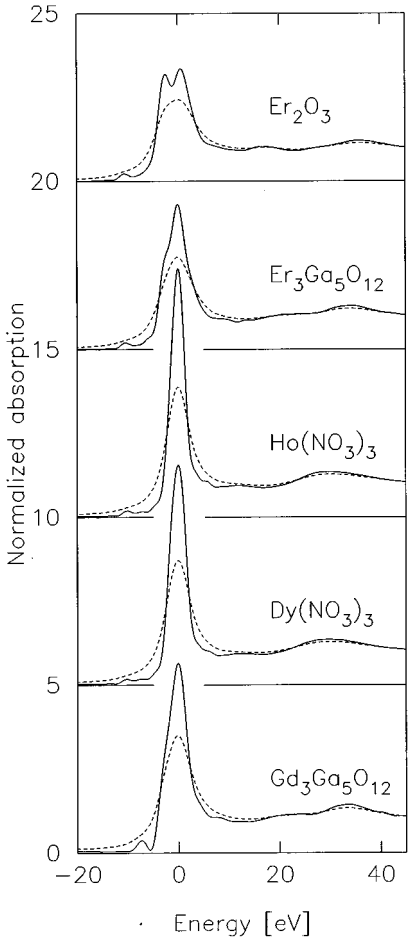

FIG. 1. The L_{III} XAS edges of five rare earth materials (dashed) coplotted with the deconvolution of the spectra by a Lorentzian of $\Gamma=3$ eV. The spectra have been offset to give coincident dipolar resonance peaks at 0 eV and the absorption has been normalized to unity at high energy.

The resolved features in Fig. 1 for Gd garnet can be corroborated by the recent resonant IXS study by Krisch *et al.*[9] They observed that the Gd white line was composed of at least two strong dipolar resonances which is seen by the enhanced asymmetry of the peak at 0 eV in the deconvolved spectrum. Furthermore, they assigned the onset of the continuum states to occur 7.5 eV above the dipolar resonance peak (7255 eV) which coincides with the appearance of a shoulder in the deconvolved spectrum. Comparable shoulders are revealed for all the spectra in Fig. 1. Also the weak pre-edge feature for Gd garnet seen in Fig. 1 corresponds in energy (7240 eV) to that observed by Krisch *et al.*[9] and exhibits the same single-peaked form.

The weak pre-edge structure illustrates the power of the deconvolution technique to reliably expose small features in the absorption. Figure 2 zooms in on the pre-edge region for four of the RE materials discussed so far. In each case, a scaled atomic multiplet calculation of the electric quadrupole absorption $|2p^6 4f^N\rangle\rightarrow|2p^5 4f^{N+1}\rangle$ is superposed on the plot. The calculations were made with Cowan's program[16] with Coulomb parameters obtained within the Hartree-Fock

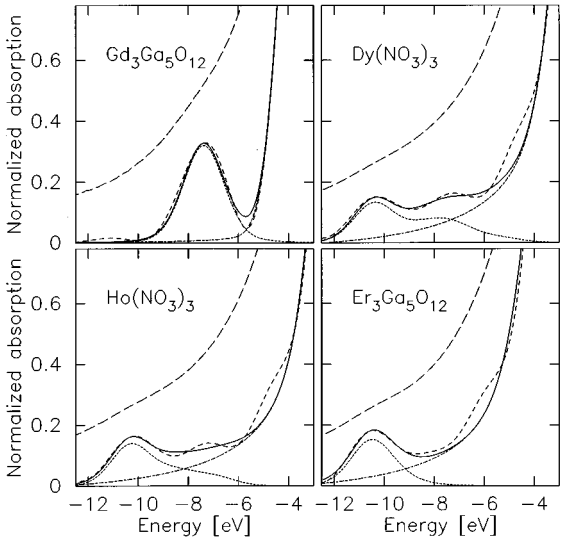

FIG. 2. Enlargements of the pre-edge region of four of the spectra in Fig. 1. The curves are (i) XAS data (long dashed line), (ii) XAS deconvolved by $\Gamma=3$ eV (medium dashed line), (iii) atomic multiplet calculations of $2p\rightarrow 4f$ absorption (dotted line), (iv) tails of the function fitted to the dipolar resonances (dash-dotted line), and (v) the sum of (iii) and (iv) (solid line).

limit reduced to 80% to account for intra-atomic screening effects. The calculated quadrupolar XAS spectra were added to the tails of models of the larger dipolar resonances and scaled to give the best agreement with the deconvolution. The dipole resonances were modeled by least squares fitting a curve composed of the sum of two Voigt functions expressed in an algebraic form.[17] The separation of the fitted peaks in the dipolar resonance was 2.6, 1.7, 1.4, and 2.6 eV for the Gd, Dy, Ho, and Er compounds shown in Fig. 2. The fitting of the dipole peaks made it possible to determine experimentally the ratio of the sums of the oscillator strengths for the quadrupolar and dipolar resonances by comparing the integrated spectral intensities. The ratios were 2.6%, 2.0%, 1.6%, and 1.4% for the Gd, Dy, Ho, and Er spectra, respectively. A value of 1.8% was quoted by Krisch *et al.*[9] for Gd garnet for the ratio of the peak heights. In each case, the absolute value of the dipolar integrals were equivalent to within 10% but the quadrupolar integrals decreased in strength with increasing atomic number Z following the ratio 7:5.2:4.2:3.5 (Gd:Dy:Ho:Er). This closely reproduces the ratio 7:5.3:4.4:3.4 (Gd:Dy:Ho:Er) of the number of unoccupied $4f$ electronic states in the respective RE atoms when normalized by $(Z\alpha)^2$ (where $\alpha=1/137$ is the fine structure constant). The term $(Z\alpha)^2$ comes from the ratio of the quadrupolar-dipolar transition probabilities.

The model spectra in Fig. 2 (solid lines) closely resemble the deconvolved XAS spectra. The small oscillatory deviations, e.g., for the Ho spectrum between -9 and -6 eV, are commensurate with the 1% error discussed earlier in this paper. The spectra are in agreement to within this margin which indicates that the shoulders observed at -5 eV in the Dy and Ho spectra and at -6 eV in the Er spectra are significant. We can offer no explanation for this new structure. Figure 2 shows that the deconvolution technique may be used to obtain unique information on $2p\rightarrow 4f$ quadrupolar

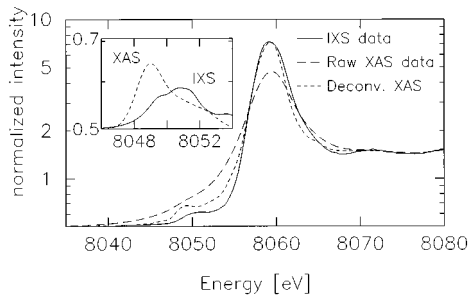

FIG. 3. IXS measurement (self absorption corrected) of $Ho(NO_3)_3$ analyzing a constant emission energy (solid line) coplotted with the raw XAS data (long dashed line) and the XAS spectrum deconvolved by a Lorentzian of $\Gamma=2.3$ eV. The inset shows the calculated $2p\rightarrow 4f$ quadrupolar XAS spectrum (dashed line) compared to the calculated quadrupolar part of the IXS spectrum. All plots are shown in logarithmic scale (after an intensity offset of 0.5) for clarity of presentation.

absorption. We note that dipolar $3d\rightarrow 4f$ absorption (M_{IV} and M_{V} XAS) is not in general the same.

We now contrast the deconvolution procedure with our results from IXS of $Ho(NO_3)_3$. Figure 3 shows the IXS spectrum measured by analyzing a 0.3 eV band of the emission spectrum at constant emission energy ($\sim$7911 eV) as a function of the incident energy. Coplotted is the deconvolved XAS spectrum with Γ set to 2.3 eV such that the two spectra have equivalent dipolar peak amplitudes thereby facilitating comparison of the two curves. Although it broadly reproduces the deconvolved spectrum, the IXS spectrum lacks some structure at 8064 eV and the pre-edge feature is weaker and offset by $\sim$1.7 eV. Due to the scan taken in the IXS measurement, the effective broadening is a combination of that for the intermediate states (with a $2p$ hole) and the narrower broadening of the final states (with a $4d$ hole). However, the spectral line shape is also a combination of intermediate and final state structure and cannot be regarded as the XAS spectrum with a reduced lifetime broadening. This point is illustrated by the inset of Fig. 3 in which the atomic multiplet calculation of the electric quadrupolar absorption $|g\rangle=|2p^6 4d^{10}4f^N\rangle\rightarrow|n\rangle=|2p^5 4d^{10}4f^{N+1}\rangle$ with an artificially reduced lifetime broadening is compared with a resonant IXS calculation. In the latter calculation, interference effects between the intermediate states $|n\rangle$ and the final states $|f\rangle=|2p^6 4d^9 4f^{N+1}\rangle$ are taken into account, such that the cross section is given by[11,18]

$$\mathcal{J}(\omega,\omega')=\frac{\Gamma}{\pi}\sum_f\left|\sum_n\frac{\langle f|D^{(1)}n\rangle\langle n|D^{(2)}|g\rangle}{\omega+E_g-E_n+i\Gamma/2}\right|^2\times\delta(E_g+\omega-E_f-\omega'). \quad (2)$$

where $D^{(L)}$ denotes the components of the electric 2^L-pole operator and E_g, E_n, and E_f are the energies of the ground, intermediate, and final states, respectively. The solid line spectrum in the inset of Fig. 3 is obtained by varying the incoming photon energy ω while keeping the energy of the outgoing photon ω' fixed at the energy of the IXS experi-

mental measurement. The calculation reproduces the peak offset of ~ 1.7 eV. Indeed there is no fixed ω' trajectory through the calculated resonant IXS surface which completely reproduces the quadrupolar XAS spectrum.

In summary, we have shown that partial deconvolution of the lifetime broadening from high quality XAS spectra is viable. We have applied it to the L_{III}-edge spectra of some RE compounds and have demonstrated that the revealed structure is genuine to within 1%. The procedure resolves the smeared ligand field splitting of the L_{III} dipolar resonances. The hidden $2p \rightarrow 4f$ quadrupolar pre-edge resonances of the RE compounds have also been exposed permitting direct comparisons with atomic multiplet calculations of the quadrupolar absorption. The excellent agreement allows the quadrupolar/dipolar oscillator strength ratios to be experimentally determined. Finally, we have employed the deconvolved data of $Ho(NO_3)_3$ to assess experimentally the ability of IXS measurements at fixed ω' to reproduce the absorption with a reduced lifetime broadening.

We confirm the theoretical findings[10,11] that IXS measured with fixed ω' cannot, in general, be interpreted as the XAS spectrum. However in materials with unoccupied broadbands this may be possible and can now be verified via deconvolution of the XAS. We note that resonant IXS measured at fixed energy transfer $(\omega - \omega')$ may be used to isolate individual resonances whose decay channels are separated in ω' by more than the core hole lifetime but that this does not result in the elimination of the lifetime broadening. By contrast, the deconvolution of a Lorentzian response function from XAS spectra reveals resonances with a dramatically reduced lifetime broadening. The deconvolution procedure is a hitherto unexploited method of directly exposing absorption structure otherwise concealed by lifetime broadening which can be widely applied in XAS where good data quality is available.

We acknowledge J. Jensen and M. Kocsis for invaluable technical assistance and G. Balakrishnan for samples. All beam time was at the European Synchrotron Radiation Facility under proposal MI-83 and in-house research time.

[1] M. O. Krause and J. H. Oliver, J. Chem. Phys. Ref. Data **8**, 329 (1979).

[2] D. Gibbs, D. R. Harshman, E. D. Isaacs, D. B. McWhan, D. Mills, and C. Vettier, Phys. Rev. Lett. **61**, 1241 (1988).

[3] J. P. Hannon, G. T. Trammell, M. Blume, and D. Gibbs, Phys. Rev. Lett. **61**, 1245 (1988).

[4] G. Schütz, M. Knülle, R. Wienke, W. Wilhelm, W. Wagner, P. Kienle, and R. Frahm, Z. Phys. B **73**, 67 (1988).

[5] J. C. Lang, S. W. Kycia, X. Wang, B. N. Harmon, A. I. Goldman, D. J. Branagan, R. W. McCallum, and K. D. Finkelstein, Phys. Rev. B **46**, 5298 (1992).

[6] P. Carra, B. N. Harmon, B. T. Thole, M. Altarelli, and G. A. Sawatzky, Phys. Rev. Lett. **66**, 2495 (1991).

[7] J. C. Lang, G. Srajer, C. Detlefs, A. I. Goldman, H. König, X. Wang, and B. N. Harmon, Phys. Rev. Lett. **74**, 4935 (1995).

[8] K. Hämäläinen, D. P. Siddons, J. B. Hastings, and L. E. Berman, Phys. Rev. Lett. **67**, 2850 (1991).

[9] M. H. Krisch, C. C. Kao, F. Sette, W. A. Caliebe, K. Hämäläinen, and J. B. Hastings, Phys. Rev. Lett. **74**, 4931 (1995).

[10] S. Tanaka, K. Okada, and A. Kotani, J. Phys. Soc. Jpn. **63**, 2780 (1994).

[11] P. Carra, M. Fabrizio, and B. T. Thole, Phys. Rev. Lett. **74**, 3700 (1995).

[12] W. Drube, R. Treusch, and G. Materlik, Phys. Rev. Lett. **74**, 42 (1995).

[13] C. E. Shannon and W. Weaver, *The Mathematical Theory of Communication* (University of Illinois Press, Urbana, IL, 1963), p. 100; J.F. Young, *Information Theory* (Butterworth, London, 1971), p. 87.

[14] W. Pies and A. Weiss, in the *Crystal Structure Data of Inorganic Compounds*, edited by K. H. Hellwege and M. Hellwegea, Landolt-Börnstein, New Series, Group III, Vol. 7, Pt. E (Springer-Verlag, Berlin, 1980)

[15] F. M. F. de Groot, J. Electron. Spectrosc. Relat. Phenom. **67**, 529 (1994).

[16] R. D. Cowan, *The Theory of Atomic Structure and Spectra* (University of California Press, Berkeley, 1981).

[17] C. M. Teodorescu, J. M. Esteva, R. C. Karnatak, and A. El Afif, Nucl. Instrum. Methods A **345**, 141 (1994).

[18] M. A. van Veenendaal, P. Carra, and B. T. Thole, Phys. Rev. B (to be published).